

ASSOCIATED PRODUCTION of LEPTON and JETS

UA1 Collaboration, CERN, Geneva, Switzerland

Aachen-Amsterdam(NIKHEF)-Annecy(LAPP)-Birmingham-CERN-

Harvard-Helsinki-Kiel-London(QMC)-Paris(CDF)

Riverside-Rome-Rutherford Appleton Lab.-Saclay(CEN)-

Vienna-Wisconsin Collaboration

(Presented by M.N. Minard)

ABSTRACT

A clean signal has been observed for the production of an isolated large-transverse-momentum lepton in association with two jets. The rate and feature of these events are not consistent with expectation from known quark decays (charm, bottom). There are consistent as being the manifestation of t-quark decay, t being the sixth quark from Cabibbo current, through 2 processes $W \rightarrow t\bar{b}$ or $p\bar{p} \rightarrow t\bar{t}$, followed by semi-leptonic decay of the t-quark. That interpretation bounds the mass of the top quark in the range $30 < m_t < 50 \text{ GeV}/c^2$.

1. Introduction

In this Symposium the UA1 Collaboration has reported the observation of 201 events from $e^\pm \nu_e$ decays of the Intermediate Vector Boson (IVB) and 42 events from its muonic decay, for an integrated luminosity of 390 nb^{-1} . These events are easily recognized in the UA1 apparatus from their clean signature: association of a lepton

of high transverse momentum $E_{\perp l} \sim 40 \text{ GeV}$ and a neutrino ν_l , whose transverse energy is measured with a resolution of a few GeV; more, these W decays mode are background free and only loose criteria for electron identification are needed to identify such events.

The observation of electronic and muonic decay modes of IVB has provided an understanding of production process, particularly has shown that the expectation from QCD of initial bremsstrahlung are in agreement with the data, the jets being emitted along the incoming beam direction. The following step has been to look for other W decay signature, in particular for quark decay mode of W.

We have search for $W \rightarrow t\bar{b}$, t being the sixth quark, the top. Such a process should be observed provided that $m_T < m_W - m_b$, where m_T is the "top" mass and m_b the b mass.

From unsuccessful search of t-quark in e^+e^- colliding rings, a lower mass limit had been established for quark t, $m_T > 22 \text{ GeV}/c$.

In [1] it has been reported by the UA1 Collaboration the observation of 6 events possibly coming from semi-leptonic decay of t quark (3 electron decay, 3 muon decay). These events were compatible with the hypothesis $W \rightarrow t\bar{b}$, with a top mass in the 30 to 50 GeV range.

A similar analysis is reported here corresponding to an enlarged sample. We tried to identify $W \rightarrow t\bar{b}$ through the semi-leptonic decay mode $t \rightarrow l\nu_l b$, where l =electron or muon; that channel is chosen for a typical signature, it provides : a lepton of high p_{\perp} , two jets and some transverse missing energy. These events are expected to show several characteristics which will permit to identify and separate them from other sources of background:

- the t-quark (unobserved at PETRA) is expected to be heavy $M_T > 22 \text{ GeV}$, therefore in its decay $t \rightarrow l\nu b$ the lepton is expected to be emitted far from the b-jet, and should appear as well isolated.

- the recoiling \bar{b} -jet should have a characteristic Jacobian peak in the transverse energy distribution.
- the invariant mass ($b\nu_{\perp}$) system must be compatible with a common value : M_t .
- the invariant mass ($b\nu\bar{b}$) is expected to peak around the W mass.

The search has been done for isolated lepton of large transverse energy, associated to 2 jets (cf. fig. 1). Such requirements will accept between 20% and 25% of $W \rightarrow t\bar{b}$ ($t \rightarrow l\nu_l b$) for a top mass in the range 25-50 GeV. The number of expected events being low for muon as for electron channel (3-4 events) leads to the following remarks:

- Muon and electron channel are used, the significance of the observation relies in the existence of both channels.
- The electron (section 2) as well as the muon identification (section 3) have to use the full detector feature in order to improve the signature. The searched event topology requires jet activity, therefore QCD associated backgrounds are enhanced; the estimate of such background is included in section 2 for the electron sample. In section 4 discussion of background from known heavy quark decays ($b\bar{b}, c\bar{c}$) shows that it is not a major background source. Finally, in section 5 events interpretation discussion leads to interpret these *lepton + 2jets* events as coming from semi-leptonic decay of t-quark through 2 process $W \rightarrow t\bar{b}$ and $p\bar{p} \rightarrow t\bar{t}$.

2. Electron sample.

2.1 Electron identification.

The electron search above a minimum transverse energy threshold is done using momentum determination from the magnetic curvature measured by the Central Detector, the electromagnetic shower counters (≥ 27 radiation length, segmented in four in depth), and the hadronic calorimeter in which an electron deposits only

a small residual energy. The electron has to fulfill the following requirements:

- A deposition of $E_{\perp} \geq 15 \text{ GeV}$ in 2 adjacents electromagnetic cells.
- A charged track of measured p_{\perp} compatible at 3σ with measured electromagnetic energy.
- Matching of track and cell in position and angle at 3σ (σ being defined from test beam data).
- A longitudinal shower profile in agreement with a pure electromagnetic shower.
- Electron has to be isolated in a cone around the electron track $\Delta R = (\Delta\eta^2 + \Delta\phi^2)^{\frac{1}{2}} < 0.7$, where ϕ is the azimuthal angle and η the pseudo-rapidity: no more than 10% of the electron energy is allowed for additional energy deposition. In addition in a smaller cone (0.4) around the electron direction, the excess of E_{\perp} from other cells as Σp_{\perp} of additional tracks should stay below a 1 GeV threshold.

The background expected consists of electron from conversions and from jet fluctuations, where superposition of charged π^{\pm} associated to π^0 's fluctuate to simulate electron signature. Conversions are removed by scanning and programm (96 conversions $\gamma \rightarrow e^+e^-$)[5]. The final electron sample consists of 43 electrons events all with an energy imbalance below 15 GeV. This leaves us with a signal of 43 events splitted into 4 topologies:

2 events e^{\pm} and no jet $E_{\perp} > 8 \text{ GeV}$

28 events e^{\pm} and 1 jet

9 events e^{\pm} and 2 jets

4 events e^{\pm} and ≥ 3 jets

where a jet is defined as cells cluster in rapidity, azimuth $\Delta R = (\Delta\eta^2 + \Delta\phi^2)^{\frac{1}{2}} < 1$, jet threshold being fixed at 8 GeV for the first jet and at 7 GeV for the following in the present analysis.

2.2 Background from QCD.

Background from jets fluctuation ($\pi^\pm + n\pi^0$) faking an electron is estimated in magnitude and shape.

The magnitude from hadronic jets background is estimated using the pion sample: isolated $\pi^\pm + n\pi^0$ have been selected from electron trigger (i.e. $\pi^\pm + n\pi^0$ deposit at least 12 GeV in the electromagnetic cells). Isolation and matching criteria used for that sample selection are similar to the electron sample selection, changing only the electromagnetic shape requirement for a minimum deposition in the hadronic calorimeter $E_{had} \geq 1 \text{ Gev}$.

From the pion sample after trigger acceptance correction, one gets the overlap $\pi^\pm + n\pi^0$ flux of $E_\perp \geq 15 \text{ GeV}$; then, for each event the probability to fake an electron is calculated from test beam measurement with superimposed π^0 . Background expectation are summarized in table I for the various topologies. For the electron + 2jets channel the expected background from the overlap source is 0.9 event, unable to explain the observed signal of 9 events [2,3].

The behaviour of kinematics distributions for electron + 2jets events is compared to the ones observed from QCD jets fluctuations (where a jet fluctuates into a π^0 or $\pi^\pm + n\pi^0$). On figure 2 is plotted for isolated $\pi^0 + 2jets$ and $e^\pm + 2jets$, $\cos \theta_{J_2}^*$ vs E_\perp^{out} , where E_\perp^{out} is the transverse energy component of the isolated $e(\pi^0)$ perpendicular to the plane formed by the $p\bar{p}$ axis and the highest $E_{\perp J_1}$ and $\theta_{J_2}^*$ is the angle between the $p\bar{p}$ axis and the lowest $E_{\perp jet}(J_2)$ in the $(e(\pi^0), J_1, J_2)$ rest frame. For the background sample, one clearly observes accumulation at large $\cos \theta_{J_2}^*$, which is the expected behaviour for jet issued from bremsstrahlung of initial state. On the contrary, for the electron sample, the plot is populated in the small $\cos \theta_{J_2}^*$, large E_\perp^{out} region. The compatibility of the 2 distributions is estimated from Kolmogorov test to be $3.5 \cdot 10^{-3}$.

On figure 3 is plotted the invariant masses $(e(\pi^0), \nu_e, J_2)$ vs $(e(\pi^0), \nu_e, J_1, J_2)$

for both $e^\pm + 2jets$ and $\pi^0 + 2jets$ samples. The distribution of (e, ν_e, J_1, J_2) peaks around the W mass, but is compatible with the background distribution (π^0, ν, J_1, J_2) with a probability of $8.5 \cdot 10^{-3}$.

Therefore QCD background from jet fluctuation is unable to explain in magnitude as in shape, the observed distributions from $e^\pm + 2jets$ events.

3. The muon sample.

Muons identification relies equally in the Central Detector and in position and angle measured from the 8 planes of the muon drift chambers.

The following requirements have to be fulfilled:

- a charged track of $p_\perp \geq 12 \text{ GeV}$ and a good quality in the central detector.
- a charged track reconstructed from 3 out of 4 possible planes hits in each of the 2 projections in the muon chambers.
- matching in position and angle
- deposition in the calorimetry along track axis should be compatible with a minimum ionising particle
- isolation in a cone of $\Delta R = (\Delta\eta^2 + \Delta\phi^2)^{\frac{1}{2}} \geq 0.4$ at 90% for charged track and 80% for calorimetry.

The sample defined is scanned to validate track measurement and to remove fake high p_\perp track from K decay. That selection leads, for an integrated luminosity of 108 nb^{-1} to the sample of 12 events already published [1]:

$6 \mu + 1jet$

$3 \mu + 2jets$

$1 \mu + \geq 3jets.$

The estimated background from punch-through and decaying hadrons is estimated to 0.2 ± 0.1 event for the $\mu + 2jets$ channel, unable to explain the $3 \mu + 2jets$ events present in our data sample.

4. Background due to beauty and charm pair production.

Looking for sources of high p_{\perp} lepton associated to 2jets, we should consider the processes involving production of heavy flavours quarks which can decay semi-leptonically ($b\bar{b}, c\bar{c}$ production). These events are expected to appear as 2jets events back to back in azimuth, the lepton from semi-leptonic decay being contained in one of the jets, and then will failed the isolation requirements of our analysis. However such processes can simulate our event topology provided the lepton is leading particle and an extra jet is produced by second order QCD processes:

$$gg \rightarrow b\bar{b}g$$

$$q\bar{q} \rightarrow b\bar{b}g$$

$$qg \rightarrow b\bar{b}q$$

To calculate such background, an inclusive measurement of muon spectrum has been done for muon of $p_{\perp} \geq 12 \text{ GeV}$. All events with a muon of $p_{\perp} \geq 12 \text{ GeV}$ and at least a jet of $E_{\perp} \geq 8 \text{ GeV}$ have been selected in 1983 data sample (108 nb^{-1}). After scanning and removing known W and Z^0 candidates, we are left with 59 events, mostly containing muons embedded in jets. After acceptance correction and removing estimated background contribution from kaons decays, the cross section for $p_{\perp\mu} \geq 12 \text{ GeV}$ is calculated and presented on figure 4, showing reasonable agreement with theoretical predictions [7-10] for large p_{\perp} muon coming from $b\bar{b}$ or $c\bar{c}$ production.

Among the selected inclusive muon events 17 are $\mu^{\pm} + 2jets$ events, with in most of the cases the muon belonging to a jet.

When isolation criteria used in our analysis are applied on Monte Carlo data (ISAJET) [6] for $b\bar{b}$ or $c\bar{c}$ production, one gets a reduction factor of 20 for μ of $p_{\perp} \geq 12 \text{ GeV}$, which leads to expect the background of ; 0.9 event coming from $b\bar{b}g$ or $c\bar{c}g$.

Interesting remark can be applied to the inclusive $\mu + 2jets$ events sample leading to estimate an even smaller background in the signal region.

On figure 5.a is shown the behaviour of the 17 $\mu + 2jets$ events in acoplanarity compared to the 12 isolated leptons + 2 jets events (9 electrons, 3 muons). We plot $\cos \theta_{J_2}^*$, where $\theta_{J_2}^*$ is the angle already defined in 2.2, versus $\Delta\phi_{\mu-J_1}$ which measures the acoplanarity of the μ compared to the highest E_\perp jet. The $\mu + 2jets$ events show jet back to the muon, and again $\cos \theta_{J_2}^*$ peaks at large $\cos \theta_{J_2}^*$ as expected if J_2 comes from initial state bremsstrahlung.

If events at large $\cos \theta_{J_2}^*$ are removed from the sample ($|\cos \theta_{J_2}^*| < 0.80$) we are left with 8 events: 3 events very well isolated and clustering in the W mass region for $M(\mu, \nu_\perp, J_1, J_2)$ which are the 3 $\mu + 2jets$ events candidates, and 5 events not isolated and flatly distribution over the whole mass range (cf. figure 6). In table II we summarized, for different kinematical cuts, the expected background from $c\bar{c}$ and $b\bar{b}$ production which in the worst case will be :

$$< 0.9 \text{ events for } \mu + 2jets \text{ } (p_{\perp\mu} \geq 12 \text{ GeV}) \text{ and } 108 \text{ nb}^{-1}.$$

$$< 1.3 \text{ events for } e + 2jets \text{ } (p_{\perp e} \geq 15 \text{ GeV}) \text{ and } 390 \text{ nb}^{-1}.$$

and then is unable to explain the 12 leptons+2jets events recorded in the present analysis.

5. Event interpretation.

To interpret the 12 events with a lepton (muon or electron) and 2 jets, we will discuss two possible origins:

$$(1) \quad p\bar{p} \rightarrow W \rightarrow t\bar{b}$$

$$(2) \quad p\bar{p} \rightarrow t\bar{t}$$

where the t-quark decay semi-leptonically.

We compare various kinematical variables to the expected distributions for different t-quark mass hypothesis. On figure 7 we show the 3-body invariant mass (l, ν_\perp, J_2) versus the 4-body invariant mass (l, ν_\perp, J_1, J_2) . In the 4-body projection,

a peak can be observed around the W mass, while the 3-body state clusters around 40 GeV. We will expect that type of behaviour for a new W decay to $t\bar{b}$. Figures 8-9 show different kinematics quantities of the observed events compared to the expected distribution from ISAJET Monte Carlo. All these distributions show reasonable agreement with the hypothesis $W \rightarrow t\bar{b}$ for a t -quark mass in the range 30-50 GeV. Then, so far the hypothesis $W \rightarrow t\bar{b}$ is the most likely interpretation for these events.

The expected rate of events from $W \rightarrow t\bar{b}$ process can be calculated using the most recent estimation for the W cross-section: $\sigma_{W \rightarrow e\nu_e} = 0.59 \pm 0.09[4]$.

In that hypothesis we will expect for the electron decay associated to 2 jets 3 ± 1 events for an integrated luminosity of 390 nb^{-1} , fulfilling all the analysis selection criteria (ISAJET calculation). In the electron channel we see 9 events and the various background considered so far are only able to explain 1-2 events.

We have to consider other contributions such as $p\bar{p} \rightarrow t\bar{t}$, where one of the t -quark decays semi-leptonically. Figure 10 shows, from Monte Carlo calculations with $M_t = 40 \text{ GeV}$ hypothesis (ISAJET), the expected behaviour for the typical kinematical variables already plotted for $W \rightarrow t\bar{b}$ hypothesis (cf. figure ..). From these plots we can remark that it is very difficult to distinguish between $W \rightarrow t\bar{b}$ and $t\bar{t}$ production process: all kinematic behaviours are very close in the hypothesis of t -quark mass around 40 GeV. Consequently the $t\bar{t}$ production process has to be considered. The $t\bar{t}$ production cross section being unknown we attempt to get an order of magnitude for its contribution to lepton+2jets channel:

- In 22% of the cases, the $t\bar{t}$ production will give an electron associated with more than 2 jets in the final state (ISAJET calculation), and in 45% of the cases an electron associated to 2 jets.
 - We observe 4 events with more than 2 jets for an expected background of 0.5 and an expected contribution from $W \rightarrow t\bar{b}$ of 0.5.
 - If $t\bar{t}$ production is the main source of lepton + > 2jets events, then we
-

will expect $t\bar{t}$ to contribute for twice as much events to the lepton+2jets events: the expected contribution will be of 6 events in the electron+2jets channel.

In that frame the 9 electron+2jets events will be interpreted as 40% coming from $W \rightarrow t\bar{b}$ and 60% from $p\bar{p} \rightarrow t\bar{t}$. This shows the importance of understanding $t\bar{t}$ production cross-section at the collider energy. This is still in progress through systematic studies of all its possible decay-modes.

6. Conclusion.

Events are observed containing an isolated charged lepton of high transverse energy associated with 2 jets. They cannot be due to non leptonic background.

12 events have a high p_{\perp} lepton (9 electrons, 3 muons) and 2 jets, the (*lepton* + ν_{\perp} + *jets*) mass clusterized around the W mass, showing compatibility with $W \rightarrow t\bar{b}$ hypothesis. Therefore Monte Carlo expectation for that contribution to the present analysis is only of 3-4 events, but contribution from $p\bar{p} \rightarrow t\bar{t}$ is expected not to be negligible for a t-quark mass of 40 GeV.

All kinematical distributions for observed events agree with expectation from the 2 possible processes:

$$p\bar{p} \rightarrow W \rightarrow t\bar{b} \quad \text{or} \quad p\bar{p} \rightarrow t\bar{t}$$

$$t \rightarrow e(\mu)\nu b$$

where t is the sixth quark of the Cabibbo current, for a mass of t-quark in the range $30 < m_t < 50 \text{ GeV}/c^2$, due to uncertainties in the jet energy scale[11].

The analysis is still under progress for 1984 of the muon channel and for lower energy range ($12 < E_{\perp el} < 15 \text{ GeV}$) of the electron channel.

References

- [1] UA1 Collaboration. Phys. Lett. (1984).
 - [2] M.N. Minard et al., Background study of $e + jets$ events. CERN-UA1-TN 84-77 (1984).
 - [3] Background estimate to electron- I. Wingerter (1985). Thesis.
 - [4] S. Geer This conference proceeding.
 - [5] M. Della Negra et al., Expected rate of background to the electron sample from conversion. CERN-UA1-TN/84-76 (1984).
 - [6] F.E Paige and S.D. Protopopescu. ISAJET program. BNL 29777 (1981).
 - [7] R. Horgan and M. Jacob. Nucl. Phys. B238 (1984), 221.
 - [9] F. Halzen and D.M. Scott. Phys. Lett. 129B (1983), 341.
 - [10] R. Kinnunen-University of Helsinki (1984). Thesis.
 - [11] M. Della Negra and P. Ghez. CERN UA1-TN/84-15 (1984).
-

Table I

	Predicted Background $\int Ldt = 39nb^{-1}$	Number of electrons $\int Ldt = 390nb^{-1}$
1 jet	3.2 ± 0.7	28
2 jets	1.1 ± 0.4	9
> 2 jets	0.5 ± 0.2	4

Table II

			$ \cos \theta^* < 0.8$		$ \cos \theta^* < 0.8$ $60 < M < 100$	
	N_{events}	$B\bar{B}G$	N_{events}	$B\bar{B}G$	N_{events}	$B\bar{B}G$
μ $p_{\perp\mu} > 12GeV$ $118nb^{-1}$	3	0.9	3	0.4	3	0.15
e $E_{\perp}^{el} > 15GeV$ $390nb^{-1}$	9	1.3	7	0.5	7	0.25

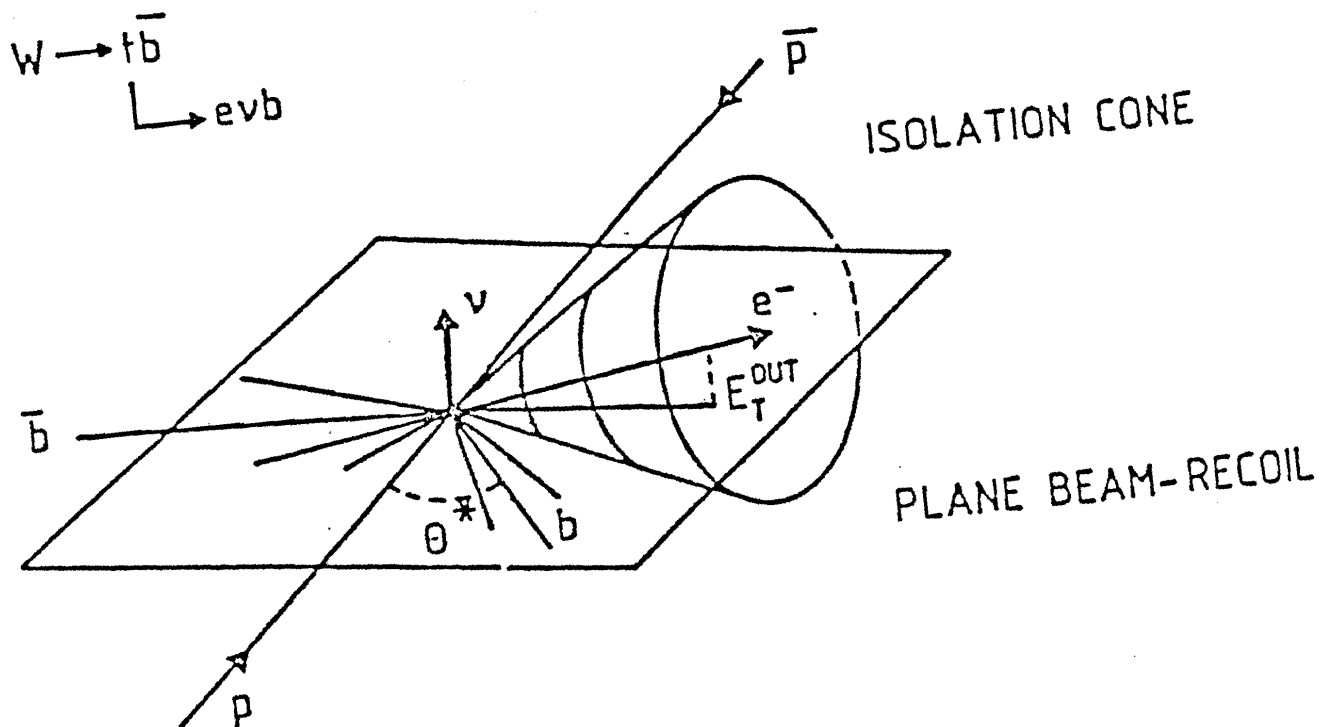


Figure 1:

The decay characteristic of $W \rightarrow t\bar{b}$ followed by $t \rightarrow e^-\nu b$ and \bar{b} will appear as 2 jets. \bar{b} -Jet is expected to show a Jacobian peak on E_T .

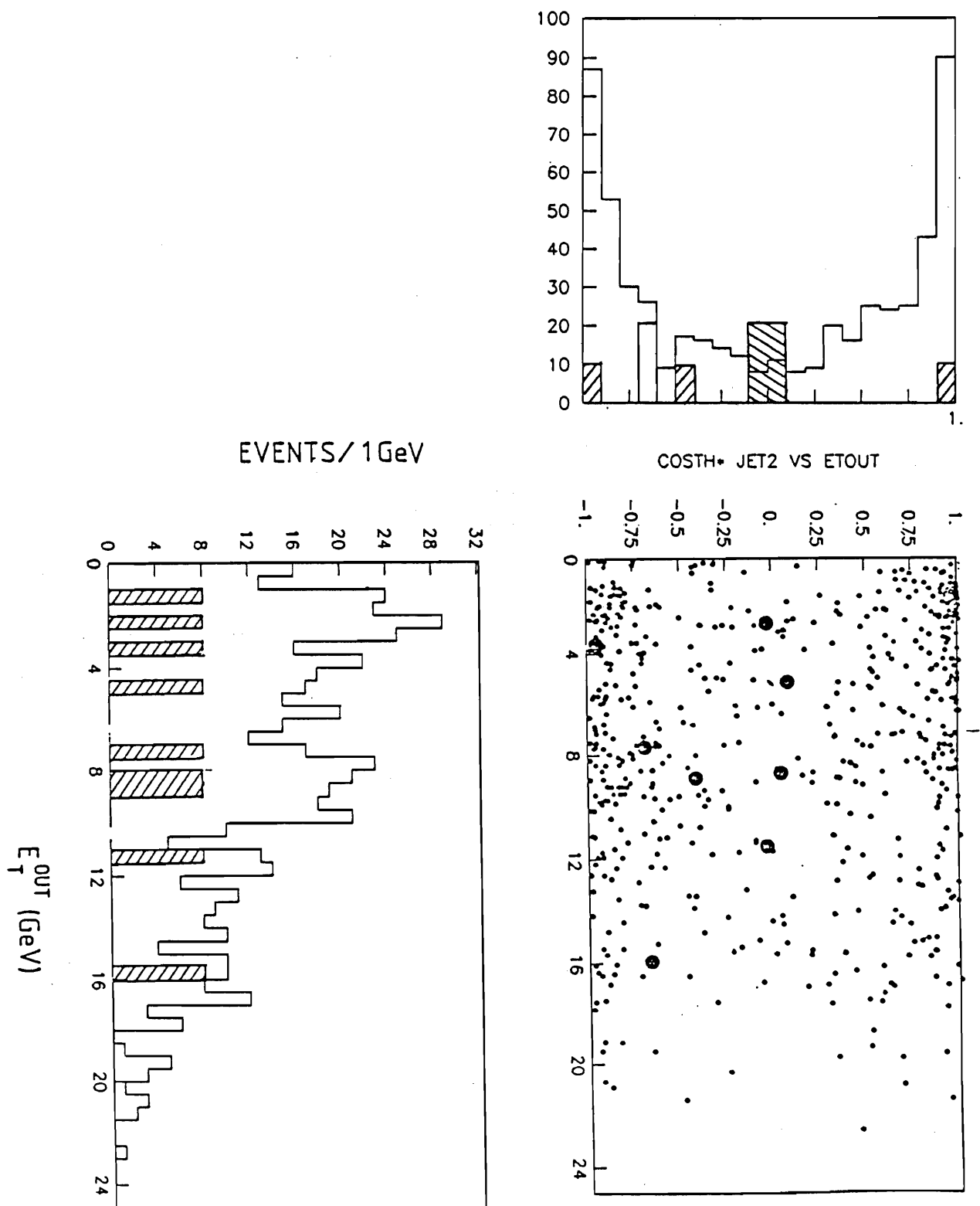


Figure 2:

Measured shape of the expected QCD background extracted from $\pi^0 + 2$ Jets events. The transverse energy component of the isolated π^0 perpendicular to the plane formed by the pp axis and highest E_{\perp} jet: E_{\perp}^{out} is plotted as a function of $\cos\theta_J^*$. The angle θ_J^* , is defined between the average beam axis in the 3-body rest frame and the lowest E_{\perp} jet (J_2). In black circles figure the 9 e+jets events.

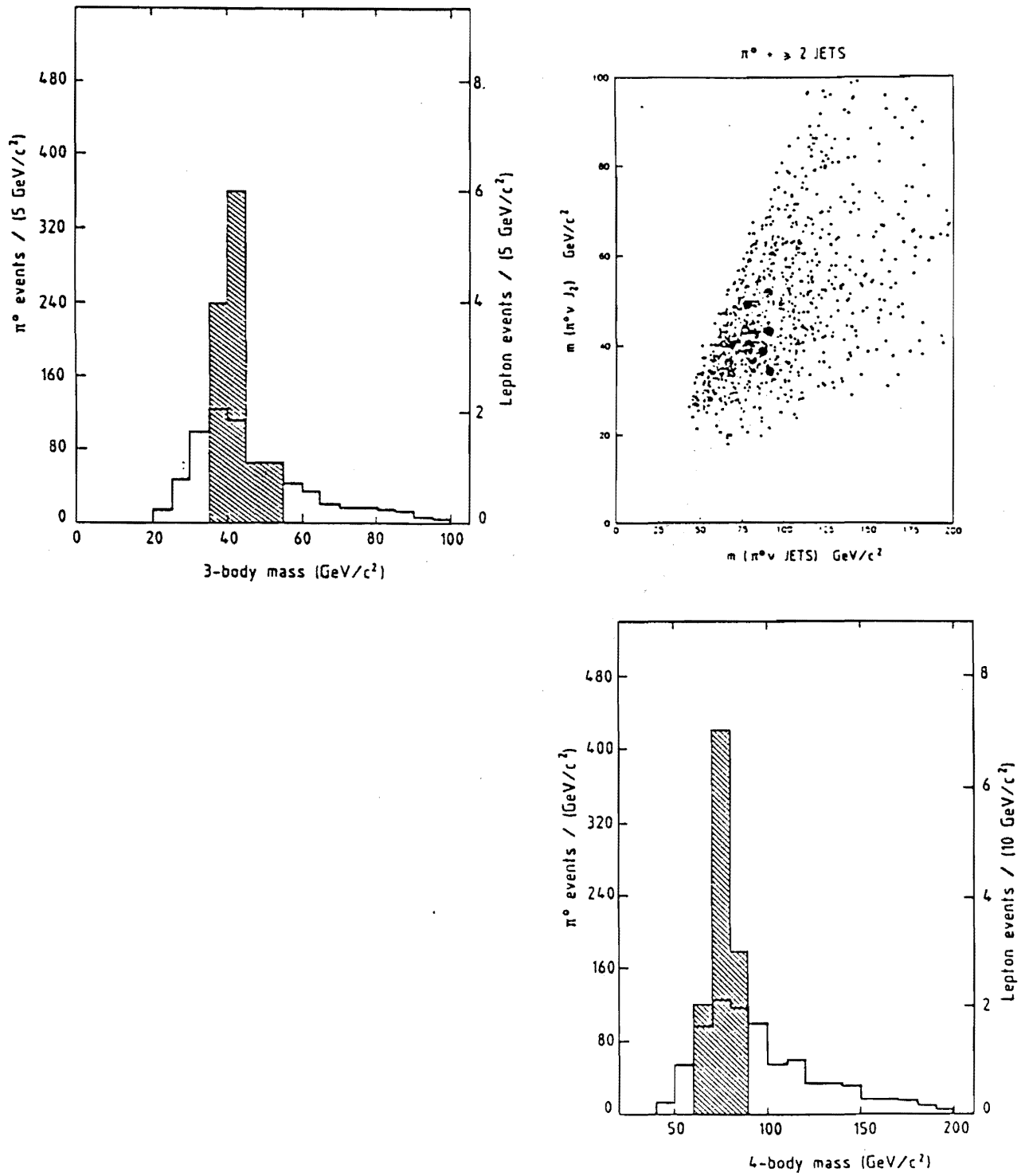


Figure 3:

Invariant mass spectrum for 3-body ($\pi^0\nu J_2$) versus 4-body ($\pi^0\nu J_1 J_2$) where J_1 and J_2 are respectively the highest and the lowest E_\perp jet in the event. Solid circles and dashed histogramms on projection figure the same distribution for the 9 e+2 jets events, normalised to the same area.

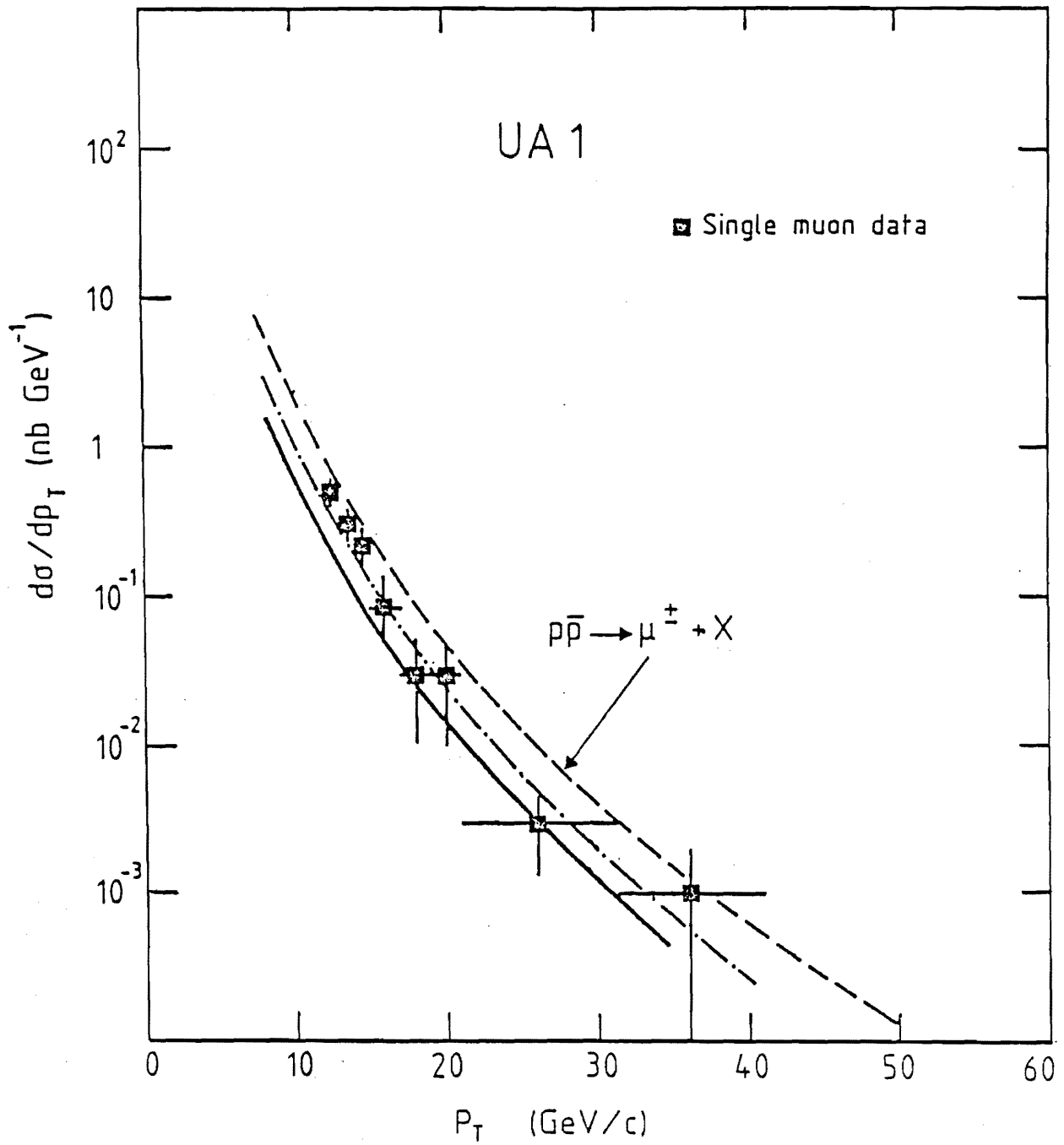


Figure 4: Measured inclusive muon p_{\perp} spectrum for $p_{\perp\mu} \geq 12\text{GeV}$ with no isolation cuts. The displayed curves are theoretical predictions of the inclusive muon rate from b and c quarks :Horgan and Jacob[7],Halzen and Scott[8](dot-dashed) and Kiinnunen [9](solid curve).

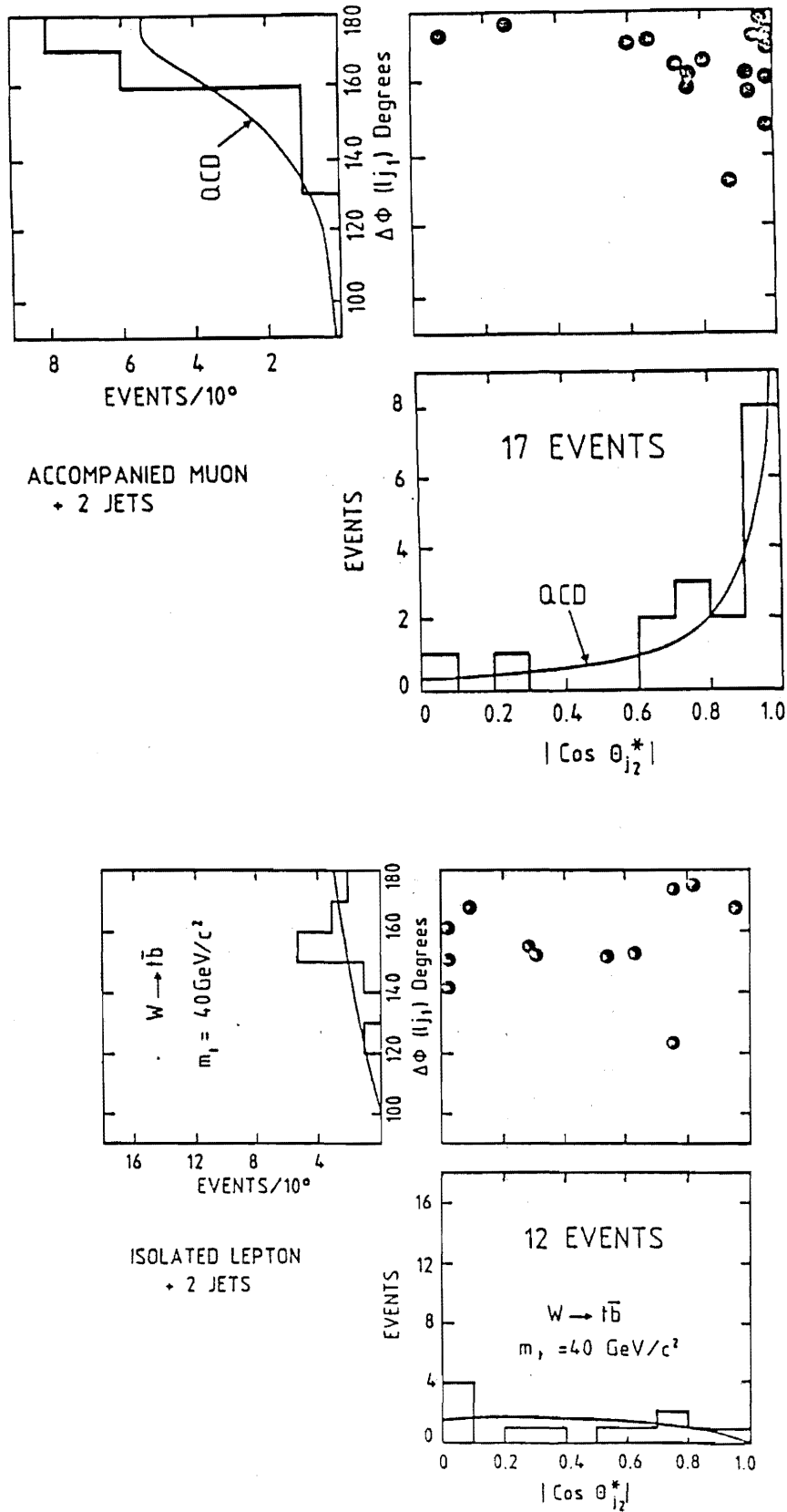


Figure 5: Lepton + 2 jets event shape : a) for the non-isolated muon sample, b) for the isolated muon and electron sample. The angle in the transverse plane between the lepton and the highest E_{\perp} jet $\phi(l - j_1)$, is shown as a function of $\cos \theta_{j_2}^*$ (see fig.2). The curves show the expectation from a) QCD background events and b) from $W \rightarrow t\bar{b}$ with a top mass $m_t = 40 \text{ GeV}$

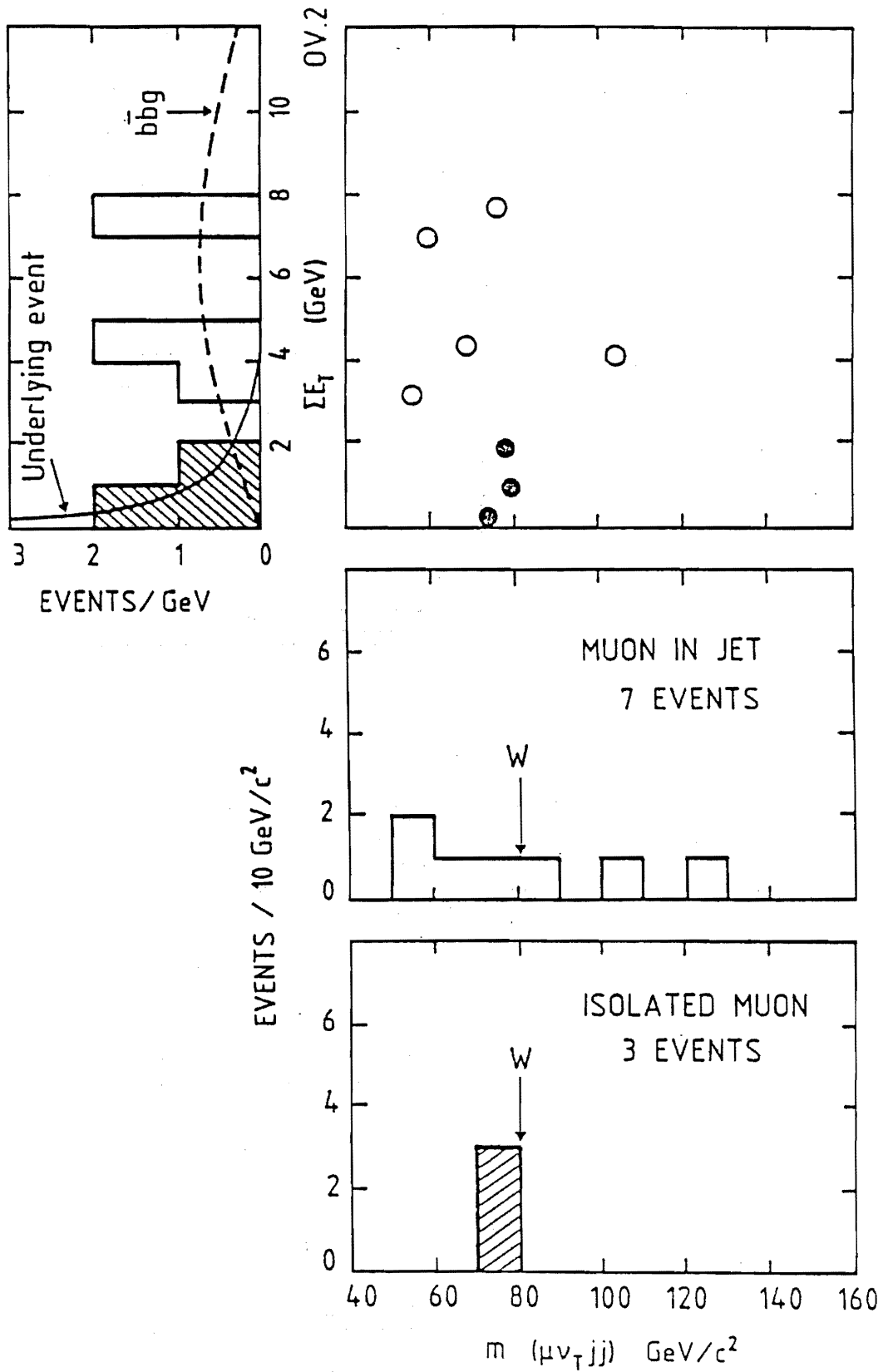


Figure 6: 4-body mass distribution for isolated muon+2 jets (dashed and full circles) and non isolated muons (empty circle) plotted as a function of additional energy deposited in a cone $\Delta R = 0.4$ around the muon. a) Isolated muons (shaded) peak at W mass. The distribution ΣE_T for the isolated events agrees with that expected for isolated muons (solid curve). The ΣE_T distribution for the non isolated events agrees with ISAJET prediction for bb and $c\bar{c}$ processes (dashed curve).

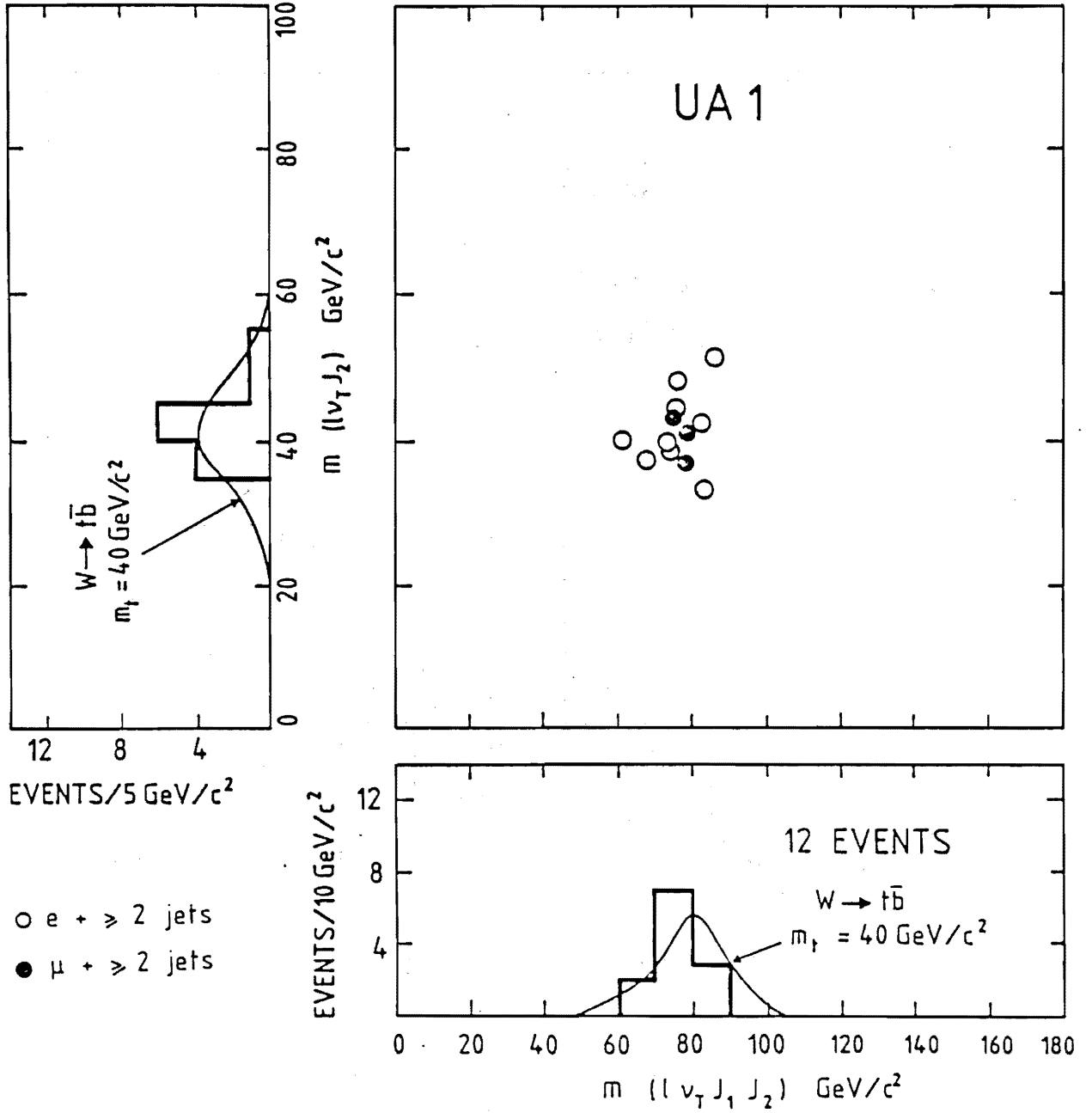


Figure 7: 4-body versus 3-body mass distribution for $W \rightarrow t\bar{b}$ candidate events. The effective mass of the lepton, the lowest E_T jet and the transverse component of the neutrino is plotted against the mass of the lepton, 2 jets and transverse neutrino system. The 4-body mass peaks at the W mass. The 3-body system clusters around $40 \text{ GeV}/c^2$. The curves show the expected distributions, taking in account the experimental resolution, for a t -quark mass hypothesis of 40 GeV .

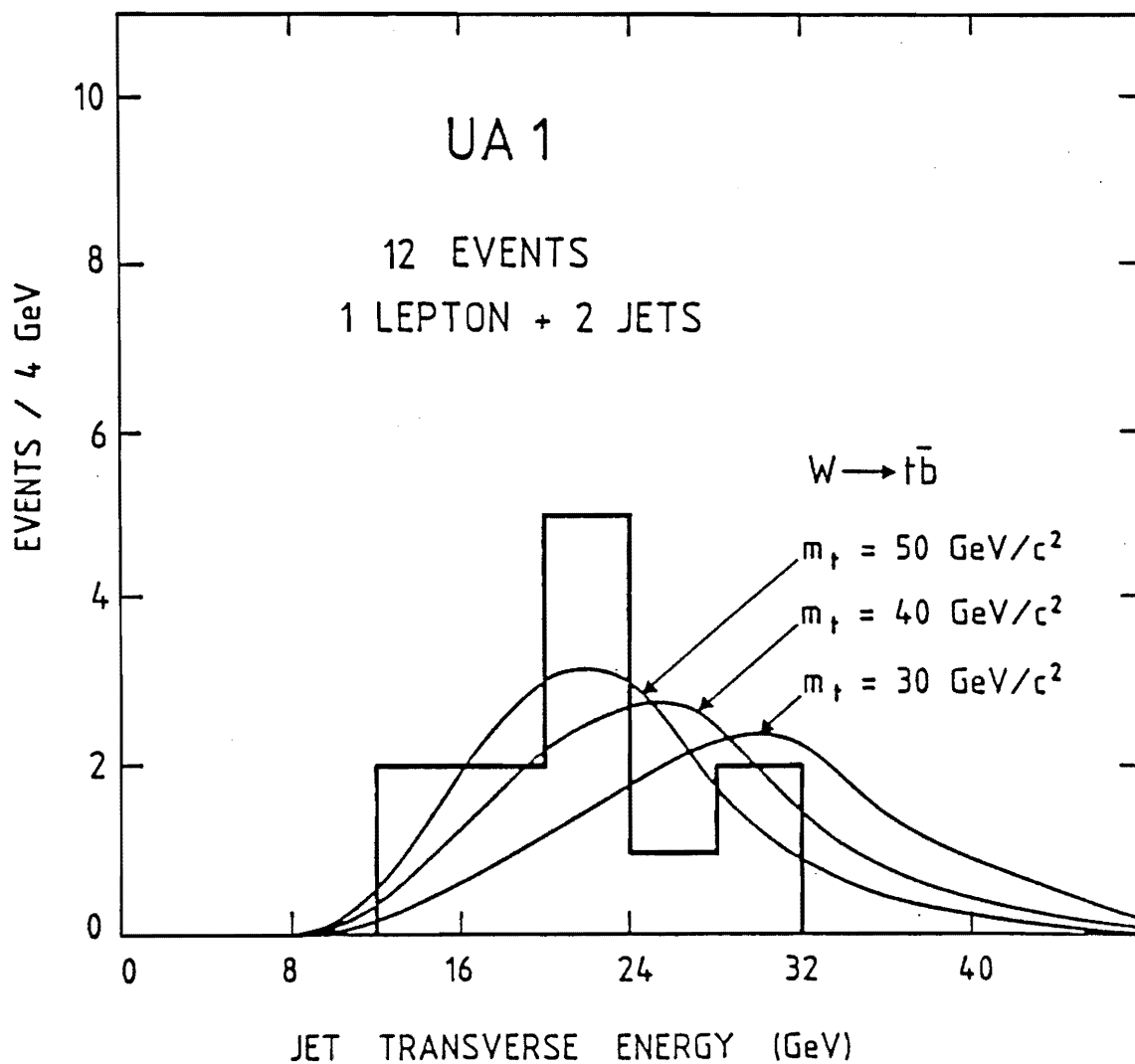


Figure 8: The jet transverse energy of the highest E_{\perp} jet is plotted. In case of $W \rightarrow t\bar{b}$ it is expected to get a jacobian peak. The curves show, taking in account the experimental resolution, the expected distribution for various t-quark mass hypothesis. The data are in agreement with these curves which are not very determinant for mass determination.

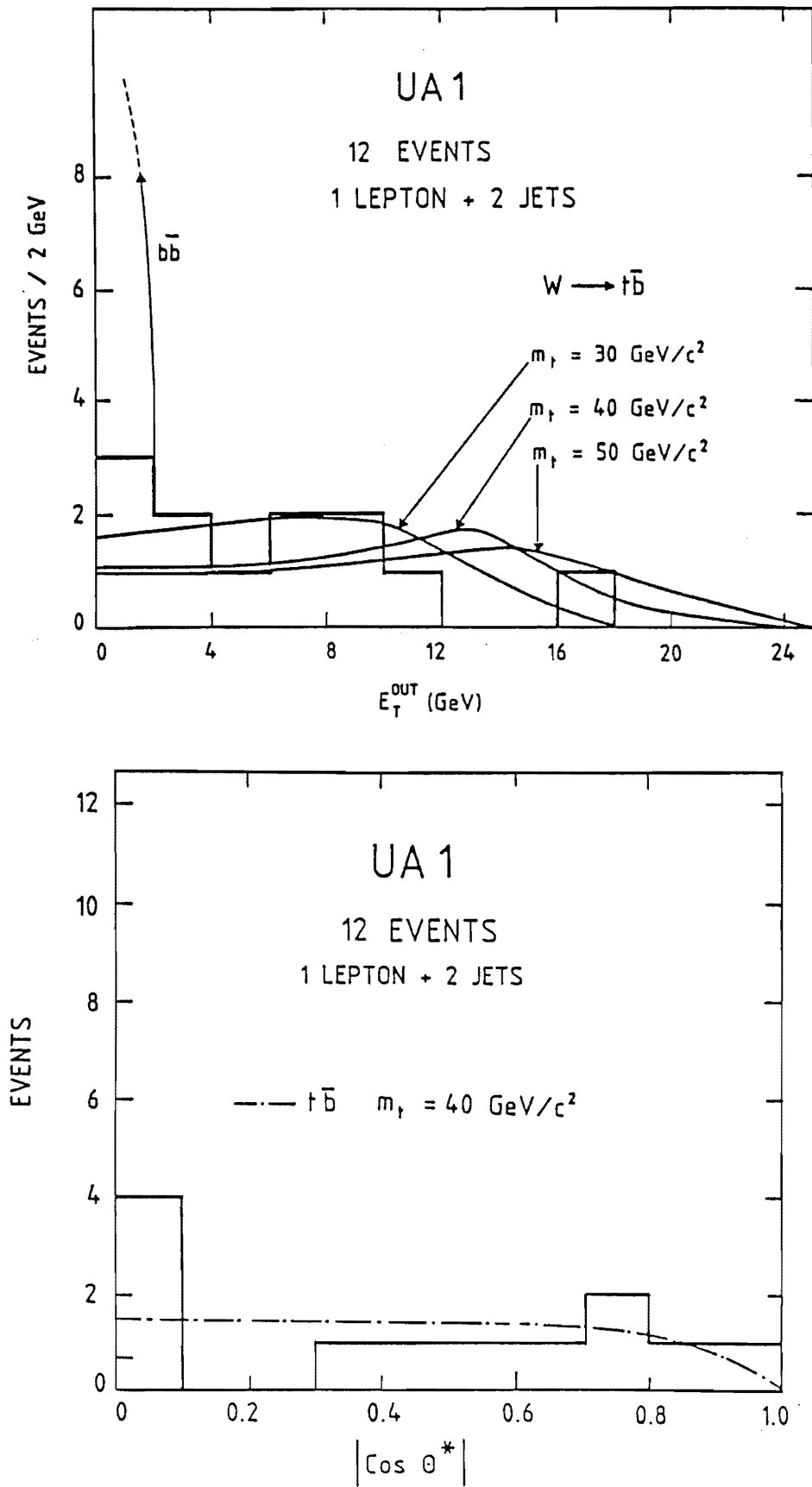


Figure 9: It is shown as well for the data than for the Monte-Carlo the expected distribution for $W \rightarrow t\bar{b}$.
a) for E_T^{out} of highest E_T jet (fig.2) b) for $\cos \theta_{J_2}^*, \theta^*$ being defined as in fig.2

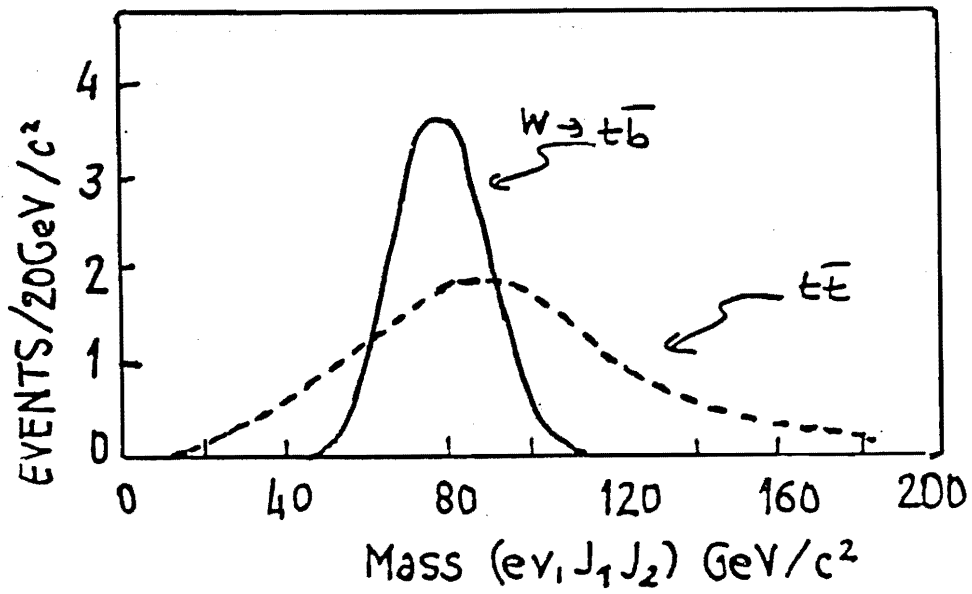
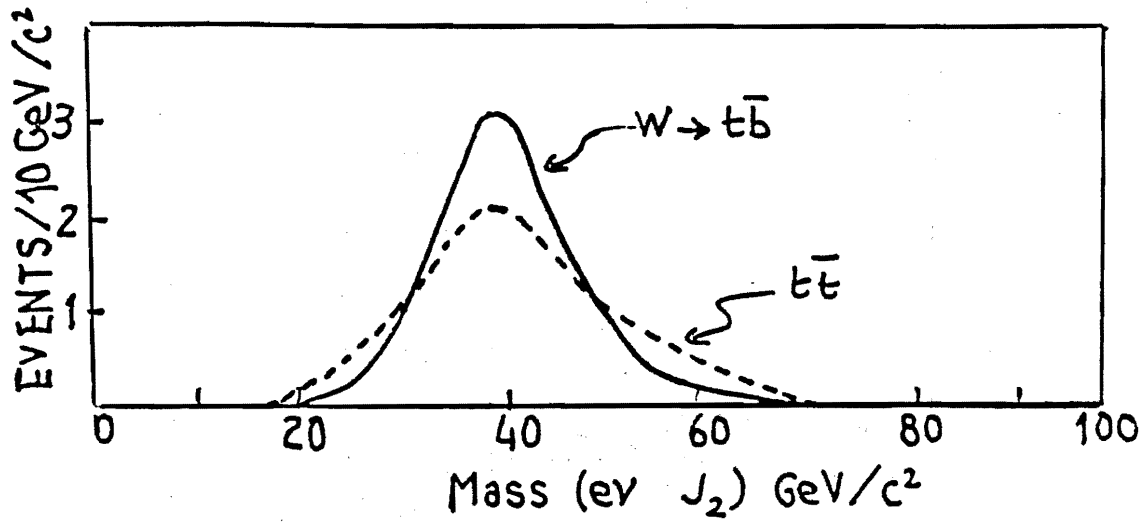


Figure 10: Invariant mass expected for $t\bar{t}$ production for 1+2 jets events (dashed) a) 3-body mass, b) 4-body mass; compared to expected distribution for $W \rightarrow t\bar{b}$ (solid curve).